

Laser-Plasma Interactions at 0.53 μm for Disk Targets of Varying Z

W. C. Mead, E. M. Campbell, K. G. Estabrook, R. E. Turner, W. L. Kruer, P. H. Y. Lee,
B. Pruett, V. C. Rupert, K. G. Tirsell, G. L. Stradling, F. Ze,
C. E. Max, and M. D. Rosen

Lawrence Livermore National Laboratory, Livermore, California 94550

(Received 23 March 1981)

Disk targets of Be, CH, Ti, and Au have been irradiated with 0.53- μm laser light in 3–30-J, 600-ps pulses, at intensities from 3×10^{13} to $\sim 4 \times 10^{15}$ W/cm². The measured absorptions, hard-x-ray fluxes, and sub-keV emission properties are compared with hydrocode simulations. The results show strong collisional absorption, some Brillouin scattering, little suprathreshold electron production, and efficient conversion of absorbed energy into sub-keV x rays, in general accord with wavelength-scaling predictions.

PACS numbers: 52.50.Jm

Many different driver- and target-design options have been proposed for achieving inertial confinement fusion. The use of submicron-wavelength laser drivers has been predicted to offer several advantages over longer-wavelength lasers.¹⁻³ With a submicron laser, energy deposition occurs in higher-density, cooler plasma and this should improve the laser-plasma coupling characteristics. The absorption region is calculated to be more collisional, increasing the inverse bremsstrahlung absorption and reducing many of the deleterious effects of plasma instabilities.^{1,3} In addition, overdense plasma heating and ablation rates should be increased,^{1,2} and the sensitivity of these rates to electron transport inhibition decreased.² However, the subtlety of competing processes makes it very important to study submicron laser-plasma interactions with use of experiments and hydrodynamic-code calculations to test these predictions.

Experiments performed at Ecole Polytechnique were the first to indicate increased absorption, enhanced thermal heating, and reduced suprathreshold-electron temperatures.⁴ More recently, other laboratories have presented further evidence for enhancement of laser-plasma coupling at shorter wavelengths.⁵ The work reported here is the first to study the interaction of submicron laser light with high- Z targets, to measure the efficiency of subsequent conversion into sub-keV x rays, and to make comparisons with detailed computer hydrodynamics calculations.

Measurements have been performed to investigate absorption, hot-electron production, and conversion of absorbed energy into sub-keV x rays. We have irradiated 600- μm -diam by 20- μm -thick disk targets of Be, CH, Ti, and Au with 600-ps near-Gaussian pulses of 0.53- μm light from the frequency-doubled Argus Nd-glass laser.

With $f/2$ focusing optics, intensities were varied from 3×10^{13} to $\sim 4 \times 10^{15}$ W/cm² by using spot diameters of ~ 50 to 450 μm , and laser energies from 3 to 35 J.⁶

Throughout this work, we have used LASNEX⁷ one- and two-dimensional Lagrangian hydrodynamics simulations to help in understanding the basic interaction processes. The modeling used here, including non-local-thermodynamic-equilibrium atomic physics, single-group thermal electron transport, and multigroup flux-limited diffusion for the suprathreshold (and all laser-heated) electrons, is largely consistent with that used previously.⁸ Inverse bremsstrahlung absorption is calculated by using the classical absorption opacity, though some nonlinear effects remain to be incorporated in the model.^{9,10} Resonance absorption^{11,12} is modeled simply by depositing a fraction, f_d , of the light approaching the critical surface into a prescribed hot-electron source. The absorption model has been extended to calculate the level of stimulated Brillouin backscatter.¹³ The amplitude of Brillouin ion waves is calculated from the evolving plasma profiles, and the backscatter is then evaluated by using a model based on theory and plasma simulations. We find that inhibited electron transport with a flux limit¹⁴ of $f_e \approx 0.03$ yields the best overall agreement with these 0.53- μm experiments.

Very complete laser energy distribution measurements were made with use of both equivalent-plane and chamber-transmission techniques. The intensity in the target plane has rms fluctuations of a factor of ~ 3 , with 5–25- μm spatial structures. Below, we present the data in terms of “nominal” intensities, together with intensity “bars” which show the range of intensities containing 60% of the incident energy.

The effects of finite spot size and diverging

plasma flow have been studied in several ways. We have ruled out large effects due to lateral conduction by performing nominal 3×10^{13} -W/cm² irradiations with both 450- and 150- μ m spots, and 3×10^{14} -W/cm² irradiations using both 150- and 80- μ m spots. No significant dependence on spot size was observed. Furthermore, using sub-keV x-ray imaging, we have observed that the transverse dimensions of the heated region are comparable to the laser spot size,¹⁴ in agreement with two-dimensional simulations of these experiments which show little lateral transport. We have found good agreement between full two-dimensional calculations and one-dimensional spherical-geometry calculations using a radius of curvature equal to 1 to 2 times the laser spot size. Thus, we have verified that lateral-conduction effects are not large in this work and have accounted for the effects of diverging plasma flows.

Absorptions measured for Be, CH, and Au disk targets at normal incidence with use of an enclosing scattered-light calorimeter are shown in Fig. 1. The absorption increases with decreasing intensity and increasing target Z , as would be expected for inverse bremsstrahlung absorption. The absorption was constant for target tilt angles of up to 30°. We observe increased absorption at 0.53 μ m compared with similar 1.06- μ m experiments. For example, gold disks irradiated at 0.53 μ m, 3×10^{14} W/cm², and 600 ps absorbed $80 \pm 5\%$, while similar 1.06- μ m experiments using 900-ps pulses obtained $53 \pm 5\%$. We find similar absorption increases for lower- Z targets, as reported by others.⁴⁻⁶

The absorptions calculated with use of LASNEX are plotted in Fig. 1. They generally agree well with the data. For the low- Z plasmas at high in-

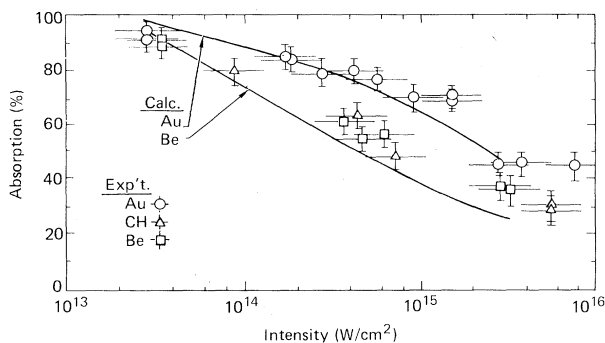


FIG. 1. Absorption results. Horizontal bars on data points indicate intensity range containing 60% of the incident energy.

tensities, some 10%–15% additional absorption (or reduced scattering) is needed to account for the measured value. If the inverse bremsstrahlung absorption calculation had included nonlinear effects,⁹ the calculated absorption for the gold disk targets at 3×10^{15} W/cm² would be similarly 10%–15% low. Simple estimates suggest that ion turbulence¹⁰ might play a significant role in contributing additional absorption. In the LASNEX absorption modeling for these experiments, we have been forced by the high-energy x-ray measurements to reduce the amount of absorption into hot electrons by decreasing the resonance-absorption dump fraction to $f_d = 0.03$. In early work using very short laser pulses at high intensity,¹⁴ $f_d = 0.3$ was motivated on the basis of simulations of resonance absorption.^{11,12} In this work, as in other recent 1.06- μ m experiments at longer pulse lengths,^{8,15} we find that the $f_d = 0.3$ model does not self-consistently reduce resonance absorption to the levels indicated by the hard-x-ray flux. Perhaps this reduction is due to longer density scale lengths near the critical surface,^{8,12} an effect not included in the model.

Experimentally, we obtain evidence for the presence of stimulated Brillouin scattering from measurements of the amount and the spectrum of the light reflected back into the $f/2$ focusing lens. For Be and CH disks at 3×10^{15} W/cm², we observe 15%–25% of the incident light reflected back into the $f/2$ focusing lens. As observed at 1.06 μ m,⁸ we find striking differences between the backscatter spectra of low- and high- Z targets. Qualitative interpretation of these spectra is elusive. However, incident-angle-dependent red shifts and increasing back reflection indicate that Brillouin scattering operates at significant levels in the highest-intensity irradiations. Simulations for the 3×10^{15} -W/cm² beryllium case show a total backscatter of 50%. This large reflectivity is obtained because the calculated scale length of the underdense plasma is ~ 100 laser wavelengths. Further work is needed to deconvolute the absorption and angular scattering processes.

We have observed the spectrum of reflected light near $\omega_{inc}/2$ to determine a lower limit for the levels of Raman side scatter.¹⁶ The energy observed in the wavelength band from 0.6 to 1.0 μ m was $\sim 10^{-5}$ of the incident energy for the highest irradiation intensities employed. We estimate that the Raman side scatter threshold is exceeded in this case by a factor of ~ 3 , and so these low levels seem reasonable.

The fluxes of 5–70-keV x rays have been measured to determine the levels of suprathermal electrons. As shown in Fig. 2(a) for Au disks, the high-energy x-ray fluence increases dramatically with increasing irradiation intensity. The spectra for disks of varying Z at $\sim 2 \times 10^{15}$ W/cm² are shown in Fig. 2(b). From the measured spectra, we infer that less than $\sim 1\%$ of the incident energy is converted into hot electrons for all target Z 's at $\sim 2 \times 10^{15}$ W/cm². The corresponding indicated "temperatures" are 9.3 ± 1.5 , 13 ± 6 , and 19 ± 7 keV for Be, Ti, and Au disk targets, respectively, at $\sim 2 \times 10^{15}$ W/cm². These levels and temperatures are the same (within uncertainties) as observed in earlier 1.06- μ m experiments¹⁷ at the same $I\lambda^2$. Thus, for fixed intensity on target, the shorter-wavelength laser produces a lower hot-electron temperature.

We have measured the characteristics of the 0.2–1.8-keV x-ray emission using three calibrated multichannel K - and L -edge filtered x-ray diode systems with subnanosecond resolving time, and a similarly filtered soft-x-ray streak camera with 15-ps resolution. We observe smoothly varying emission pulses with fall times slightly greater than the laser-pulse fall time. Within the spectral resolution ($\Delta E/E \sim 0.1$ – 0.4) of our detectors, the time-integrated x-ray spectrum corresponds closely with both previous 1.06- μ m experiments⁹ and LASNEX non-local-thermodynamic-equilibrium simulations. Other detectors show that only $\sim 3\%$ of the total radiated energy lies above 1.8 keV, and calculations imply that $\sim 90\%$ lies within the 0.2 to 1.8 keV region.

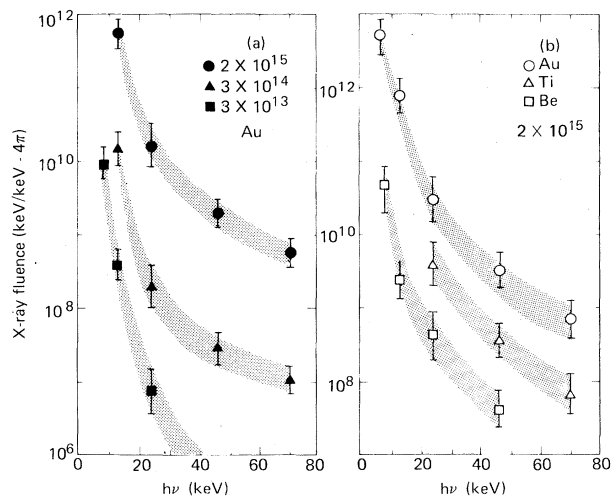


FIG. 2. Measured hard-x-ray spectra.

Using the three multiple-x-ray-diode systems which viewed the target from different angles, and using three angles of incidence (all less than 30°), we have measured the x-ray angular distribution. The integrated yields are plotted in Fig. 3 as a function of the cosine of the angle β_n between the detector and the target normal, for gold targets at 3×10^{14} and $\sim 4 \times 10^{15}$ W/cm². The LASNEX calculations reproduce the observed shift to a flatter angular distribution at $\sim 4 \times 10^{15}$ W/cm². This occurs because the 30–50- μ m spot diameter is comparable to the emission-region thickness, giving more isotropic emission than the oblate source region for the 3×10^{14} -W/cm², 150- μ m-spot irradiations.

Finally, to obtain the x-ray conversion efficiencies, we integrate over solid angle and normalize by the energy absorbed. The results, plotted in Fig. 4 for titanium and gold disks, agree well with the calculated values, except for the 3×10^{13} -W/cm² gold point, which needs further study. The conversion efficiency generally increases with increasing target Z and decreasing intensity. We can crudely see that the x-ray conversion efficiency increases as the wavelength decreases, qualitatively as predicted. For gold disks at 3×10^{14} W/cm², we obtain $50 \pm 15\%$ at $0.53 \mu\text{m}$ and 600 ps, while at $1.06 \mu\text{m}$ and 900 ps, 33% was measured.⁹

In summary, we find efficient absorption of 0.53- μ m laser light. We infer that less than $\sim 1\%$ of the incident light is absorbed into suprathermal electrons, even for Be targets at $\sim 2 \times 10^{15}$ W/cm². We have observed efficient conversion of absorbed 0.53- μ m laser light into x rays for gold disk targets. By comparison with previous 1.06- μ m experiments, we find absorption increasing, hot-electron "temperature" decreasing,

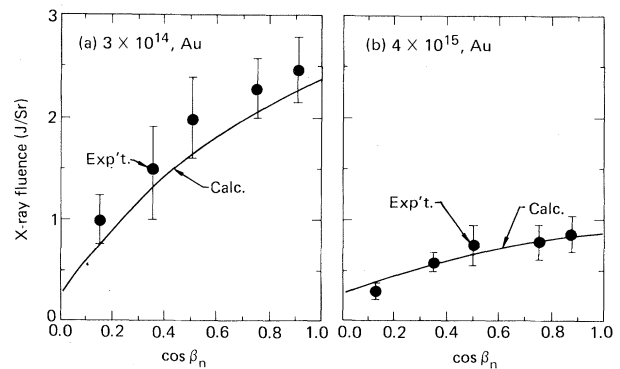


FIG. 3. Soft-x-ray angular distributions, integrated over time and photon frequency (0.1 to 1.8 keV).

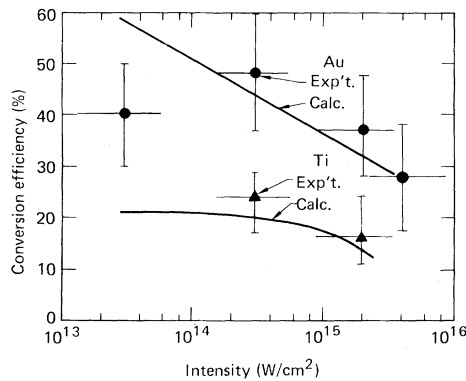


FIG. 4. X-ray conversion efficiencies ($h\nu > 0.1$ keV).

and x-ray conversion efficiency increasing as the laser wavelength decreases.

The support of J. Emmett, H. Ahlstrom, J. Nuckolls, J. Lindl, and K. Manes is appreciated. We thank B. Lesinski, D. Bailey, and G. Zimmerman for valuable contributions and discussions. The target fabrication and operations groups, and particularly W. Hatcher and G. Hermes, have helped to make these experiments successful. This work was performed under the auspices of the U. S. Department of Energy and the Lawrence Livermore National Laboratory under Contract No. W-7405-ENG-48.

¹J. Nuckolls *et al.*, *Nature (London)* **239**, 139 (1972).

²C. E. Max, C. F. McKee, and W. C. Mead, *Phys. Fluids* **23**, 1620 (1980).

³C. E. Max and K. G. Estabrook, *Comments Plasma*

Phys. Controlled Fusion **5**, 239 (1980).

⁴E. Fabre *et al.*, in *Proceedings of the Conference on Plasma Physics and Controlled Nuclear Fusion Research, Vienna, Austria, 1980* (International Atomic Energy Agency, Vienna, 1981), Paper No. IAEA-CN-38/1-4.

⁵A. G. M. Maaswinkel, K. Eidmann, and R. Sigel, *Phys. Rev. Lett.* **42**, 1625 (1979); D. C. Slater *et al.*, *Phys. Rev. Lett.* **46**, 1199 (1981); W. Seka *et al.*, *Bull. Am. Phys. Soc.* **25**, 895 (1980).

⁶E. M. Campbell *et al.*, in *Proceedings of the Fourteenth European Conference on Laser Interaction with Matter, Palaiseau, France, September 1980* (to be published); W. C. Mead *et al.*, *ibid.*; W. C. Mead *et al.*, Lawrence Livermore National Laboratory Report No. UCRL-84684 Rev. I, 1981 (unpublished).

⁷G. B. Zimmerman, Lawrence Livermore National Laboratory Report No. UCRL-75881, 1974 (unpublished); G. B. Zimmerman and W. L. Kruer, *Comments Plasma Phys. Controlled Fusion* **2**, 85 (1975).

⁸M. D. Rosen *et al.*, *Phys. Fluids* **22**, 2020 (1979).

⁹A. B. Langdon, *Phys. Rev. Lett.* **44**, 575 (1980).

¹⁰R. Faehl and W. L. Kruer, *Phys. Fluids* **20**, 55 (1977); W. M. Manheimer, *Phys. Fluids* **20**, 265 (1977).

¹¹E. J. Valeo and W. L. Kruer, *Phys. Rev. Lett.* **33**, 750 (1974); J. M. Kindel, K. Lee, and E. L. Lindman, *Phys. Rev. Lett.* **34**, 134 (1975).

¹²K. G. Estabrook, E. J. Valeo, and W. L. Kruer, *Phys. Fluids* **18**, 1151 (1975).

¹³K. Estabrook *et al.*, *Phys. Rev. Lett.* **46**, 724 (1981).

¹⁴R. A. Hass *et al.*, *Phys. Fluids* **20**, 322 (1977).

¹⁵D. L. Banner *et al.*, Lawrence Livermore National Laboratory Report No. UCRL-500-21-79, 1980 (unpublished), pp. 6-12.

¹⁶W. L. Kruer *et al.*, *Phys. Fluids* **23**, 1326 (1980); K. G. Estabrook, W. L. Kruer, and B. F. Lasinski, *Phys. Rev. Lett.* **45**, 1399 (1980).

¹⁷E. M. Campbell *et al.*, Lawrence Livermore National Laboratory Report No. UCRL-500-21-79, 1980 (unpublished), pp. 6-26.